

Volterra-series approach to stochastic nonlinear dynamics: linear response of the Van der Pol oscillator driven by white noise

Roman Belousov*

*Abdus Salam International Centre for Theoretical Physics
Strada Costiera 11, 34151, Trieste, Italy*

Florian Berger and A.J. Hudspeth

*Howard Hughes Medical Institute, Laboratory of Sensory Neuroscience,
The Rockefeller University, New York, NY 10065, USA*

(Dated: August 16, 2019/ Revision 2)

The Van der Pol equation is a paradigmatic model of relaxation oscillations. This remarkable nonlinear phenomenon of self-sustained oscillatory motion underlies important rhythmic processes in nature and electrical engineering. Relaxation oscillations in a real system are usually coupled to environmental noise, which further complicates their dynamics. Determination of the equation parameter values becomes then a difficult task. In a companion paper we have proposed an analytical approach to a similar problem for another classical nonlinear model—the bistable Duffing oscillator. Here we extend our techniques to the case of the Van der Pol equation driven by white noise. We analyze the statistics of solutions and propose a method to estimate parameter values from the oscillator’s time series.

I. INTRODUCTION

Balthazar van der Pol introduced the concept of relaxation oscillations together with his eponymous equation for a simplified dynamics of a triode electric circuit [1, 2]. Regarded as a power-series approximation for a more general class of Lienard systems [3, Sec. 7.4 and 7.5], this model became a paradigm of self-sustained oscillatory motion [2]. Besides its applications in engineering, the Van der Pol equation and its generalizations are used to describe various rhythmic processes in biology [4–12].

A general form of the Van der Pol equation that we consider in this paper extends the harmonic oscillator by introducing a nonlinear dissipative term in the equation

$$\ddot{x} + a\dot{x} + bx + c\dot{x}x^2 = f \quad (1)$$

for an unknown function of time $x(t)$ and an external force $f(t)$; the constants a , b , and c are, respectively, the friction coefficient, the stiffness, and the Van der Pol damping parameter. Because the above equation is of second order in time, the phase of this system is specified by two degrees of freedom (x, \dot{x}) .

The self-sustained oscillations of the Van der Pol equation correspond to its limit-cycle solution. In absence of the external force $f(t)$, all trajectories of this system relax to a periodic orbit in phase space. Self-sustained oscillations exist if the friction constant in Eq. (1) is negative ($a < 0$). The Van der Pol system is stable when the parameters b and c are both positive. The amplitude of the limit cycle, which encircles an unstable equilibrium point in phase space, shrinks to zero when $a = 0$ and

disappears for $a > 0$. Therefore the Van der Pol oscillator with $a \geq 0$ behaves as a monostable system. This dynamical regime is not studied in the present paper and should be treated by a different approach [13, Appendix A].

Environmental noise, which intertwines with relaxation oscillations in real systems, is often modeled by a stochastic force $f(t) = A\dot{w}(t)$, with a constant amplitude $A > 0$ and a Gaussian white noise $\dot{w}(t)$ of zero mean and unit intensity. One must usually resort to complex measures to determine the model’s parameter values for this class of stochastic nonlinear problems [9–12].

In the companion paper [13] we demonstrated that time series of a second-order dynamical system—the stochastic Duffing oscillator—contain enough information to infer the parameter values of the underlying nonlinear model. Here we extend our analysis to the case of Van der Pol relaxation oscillations driven by white noise. We derive analytical expressions for approximate solutions and time-series statistics of Eq. (1). These formulas are then used to devise a parametric method of inference.

Our approach is based on the functional series of Volterra [14, 15], which we expand up to the linear-response term. The analytical results and the inference method that we propose are therefore applicable to relatively small noise amplitudes A ; more details on the system’s physical scales are given in Sec. III. Because we must approximate the limit-cycle solution of Eq. (1), for which no closed-form expression is known, our development is restricted to moderately nonlinear regimes.

Even in the absence of external driving, the statistical properties of the relaxation oscillations are far from trivial (Appendix A). This feature of the Van der Pol equation renders the time-series analysis more difficult than in the case of the Duffing oscillator [13]. Our inference method can therefore estimate the noise amplitude

* belousov.roman@gmail.com

A only to the order of its magnitude (Sec IV).

Volterra series provide a representation of solutions for nonlinear stochastic equations. Other theoretical approaches, such as the Fokker-Planck equation and path integrals, focus instead on statistical properties of an ensemble of systems' realizations and offer less information about their dynamics. The theoretical tools may complement each other, for instance, the Volterra series may be used to an advantage in ergodic problems when time averaging is more convenient than ensemble averaging for the evaluation of statistical properties.

II. THEORY

A. Linear response of the Van der Pol oscillator

A Volterra series is a polynomial functional expansion of the form

$$\begin{aligned} x(t|f) = & x_0(t) + \int_0^t dt_1 g_1(t-t_1)f(t_1) \\ & + \iint_0^t dt_1 dt_2 g_2(t-t_1, t-t_2)f(t_1)f(t_2) + \dots \end{aligned} \quad (2)$$

in which $g_1(t)$ and $g_2(t)$ are the Volterra kernels of the linear and quadratic terms in the argument function $f(t)$. Provided that the above series exists, a truncated expansion (2) approximates solutions of Eq. (1) driven by a small external force:

$$\begin{aligned} x(t) \approx x_1(t) = & x_0(t) + \int_0^t dt_1 g_1(t-t_1)f(t_1) \\ = & x_0(t) + \gamma_1(t), \end{aligned} \quad (3)$$

in which we neglect terms of the second and higher orders in $f(t)$. The functions $x_0(t)$ and $\gamma_1(t)$ can be found by using the variational approach [13, 15, Sec. 3.4], which yields a set of equations

$$\ddot{x}_0 + a\dot{x}_0 + bx_0 + cx_0^2 = 0, \quad (4)$$

$$\ddot{\gamma}_1 + (a + cx_0^2)\dot{\gamma}_1 + (b + 2c\dot{x}_0x_0)\gamma_1 = f, \quad (5)$$

...

Equation (4), which uniquely defines $x_0(t)$ for a given initial condition $(x(0), \dot{x}(0))$, is equivalent to the homogeneous Van der Pol problem—Eq. (1) with $f \equiv 0$. The linear Eq. (5), which determines the first-order Volterra term $\gamma_1(t)$, in general contains time-dependent coefficients.

Because the Volterra series generalizes the Taylor-Maclaurin expansion of functions in calculus [15, Sec. 1.5], Eq. (2) may be restricted by a radius of convergence or may even fail to exist for some choices of $x_0(t)$. The equilibrium point $x_0(t) \equiv 0$, which is a convenient choice for the monostable case of Eq. (1), is unstable in

the regime of relaxation oscillations and yields a divergent kernel $g_1(t)$. With $x_0(t) \equiv 0$ we therefore cannot construct an approximate representation (3) that is valid for long time scales [13].

In the following the homogeneous term $x_0(t)$ represents the stable limit cycle of Eq. (4). Because a closed-form expression for this solution is unknown, as its approximation one may adopt a single-mode Fourier expansion obtained by the method of harmonic balance [16, Sec. 4.4]:

$$x_0(t) \approx \xi(t) = \alpha \cos(\sqrt{b}t), \quad (6)$$

in which $\alpha = 2\sqrt{-a/c}$. Equation (6), substituted into (5) for $x_0(t)$, yields

$$\ddot{\gamma}_1 + a_\xi \dot{\gamma}_1 + b_\xi \gamma_1 = f, \quad (7)$$

in which

$$a_\xi(t) = a + c\xi(t)^2, \quad (8)$$

$$b_\xi(t) = b + 2c\dot{\xi}(t)\xi(t) \quad (9)$$

are the time-dependent periodic coefficients. To continue the chain of simplifications, we replace the periodic coefficients in Eq. (7) by their mean values

$$\langle a_\xi(t) \rangle = \int_0^{2\pi/\sqrt{b}} \frac{\sqrt{b}dt}{2\pi} a_\xi(t) = -a, \quad (10)$$

$$\langle b_\xi(t) \rangle = \int_0^{2\pi/\sqrt{b}} \frac{\sqrt{b}dt}{2\pi} b_\xi(t) = b, \quad (11)$$

in which we relate the ensemble average of a periodic function to its time average over one period $2\pi/\sqrt{b}$. In this approximation Eq. (7) describes a harmonic oscillator $\gamma_\xi \approx \gamma_1$:

$$\ddot{\gamma}_\xi - a\dot{\gamma}_\xi + b\gamma_\xi = f \quad (12)$$

with the linear response function

$$g_\xi(t) = \Omega^{-1} \exp(at/2) \sin(\Omega t) \approx g_1(t), \quad (13)$$

in which $\Omega = \sqrt{b^2 - a^2/4}$. If $\Omega^2 < 0$ one should use $\sqrt{a^2/4 - b^2}$ instead of Ω and replace the trigonometric sine in Eq. (13) by the hyperbolic one [17, 18, Sec. II-3].

The approximate solution of the stochastic Van der Pol equation (1) is thus expressed by a sum of two *independent* contributions [Eqs. (3), (6), and (13)]

$$x(t) \approx x_\xi = \xi(t) + \gamma_\xi(t) = \xi(t) + \int_0^t ds g_\xi(t-s)f(s). \quad (14)$$

The linear-response term $\gamma_\xi(t)$ in the above equation has a Gaussian probability density, with a zero mean $\langle \gamma_\xi \rangle = 0$ and an autocovariance function [17]

$$\begin{aligned} \langle \gamma_\xi(0)\gamma_\xi(t) \rangle = & -\frac{A^2}{2ab} \exp\left(\frac{at}{2}\right) \\ & \times \left[\cos(\Omega t) - \frac{a}{2\Omega} \sin(\Omega t) \right]. \end{aligned} \quad (15)$$

Even without external driving $f(t)$, the relaxation oscillations of Eq. (1) have nontrivial statistics that are accurately described by the approximate solution $\xi(t)$ (Appendix A). Because the covariance $\langle \xi(t)\gamma_\xi(t') \rangle = 0$ of the two independent contributions $\xi(t)$ and $\gamma_\xi(t)$ vanishes, one easily obtains from Eqs. (6), (14), and (15) the autocorrelation function:

$$\begin{aligned} \chi(t) &= \frac{\langle x(0)x(t) \rangle}{\langle x^2 \rangle} \approx \chi_\xi(t) = \frac{\langle x_\xi(0)x_\xi(t) \rangle}{\langle x_\xi^2 \rangle} \\ &= \lambda \cos^2(\sqrt{b}t) + (1 - \lambda) \exp\left(\frac{at}{2}\right) \\ &\quad \times \left[\cos(\Omega t) - \frac{a}{2\Omega} \sin(\Omega t) \right], \quad (16) \end{aligned}$$

in which $\lambda = \frac{\alpha^2}{2\langle x_\xi^2 \rangle}$. The approximate autocorrelation function $\chi_\xi(t)$ is one of our main results.

B. Parametric inference

The approximate solution $x_\xi(t)$ is limited to small noise amplitudes not only due to the truncation error in Eq. (2). When the external force is strong enough to drive the system's trajectory through or very close to the special point $(x, \dot{x}) = (0, 0)$, the phase of the periodic term $\xi(t)$ can be shifted by an angle ϕ : $\xi(t) \rightarrow \xi(t + \phi)$.

As in the case of the stochastic Duffing oscillator [13], we circumvent the above issue by applying Eq. (14) *locally*: the trajectory of $x(t)$ can be split into pieces $x_+(t)$ and $x_-(t)$ for respectively $x(t) > 0$ and $x(t) < 0$. The duration of each component corresponds approximately to a half period π/\sqrt{b} of $\xi(t)$.

The above phase shifts which are not taken into account by Eq. (14), also decorrelate the time series of $x(t)$. The persistent periodic term $\propto \cos^2(\sqrt{b}t)$ in Eq. (16) is therefore accurate only at small time scales. Unlike $\chi_\xi(t)$, the actual autocorrelations of $x(t)$ decay to zero for $t \rightarrow \infty$ unless $f(t) \equiv 0$. For small amplitudes A the function $\chi_\xi(t)$ approaches its first zero as $t \rightarrow \tau \approx \pi/(2\sqrt{b})$. We may then apply the criterion of Lagarkov and Sergeev [17, 19] to select the interval $0 \leq t \leq \tau$ over which Eqs. (14) and (16) are expected to be accurate.

Although Eq. (16) predicts accurately the initial decay of $\chi(t)$ (Sec. IV), fitting this expression to autocorrelations of the time series $x(t)$ overestimates the absolute magnitude of the parameter a . As noted in the companion paper [13], the value of a is sensitive to errors of the approximations used. In Appendix C we propose therefore a correction formula

$$\begin{aligned} \chi(t) \approx \bar{\chi}(t) &= \lambda \cos^2(\sqrt{b}t) + (1 - \lambda) \exp\left(-\frac{\bar{a}t}{2}\right) \\ &\quad \times \left[\cos(\bar{\Omega}t) + \frac{\bar{a}}{2\bar{\Omega}} \sin(\bar{\Omega}t) \right], \quad (17) \end{aligned}$$

in which $\bar{a} = -a[1 + (5/16)a^2/b]$ and $\bar{\Omega} = \sqrt{b^2 - \bar{a}^2/4}$.

Equations (14) and (17) are sufficient to implement a simple technique of parametric inference. First one can fit empirical autocorrelations of $x(t)$ by $\bar{\chi}(t)$ over the time interval $0 \leq t \leq \tau$ and thus determine the parameter values a and b . Considering $\gamma_\xi(t)$ in Eq. (14) as a Gaussian error term, one may then fit the trajectory pieces $x_\pm(t)$ by

$$\xi(t - t_0) = \alpha_c \cos(\sqrt{b}t) + \alpha_s \sin(\sqrt{b}t), \quad (18)$$

in which the unknown parameter values

$$\alpha_c = \alpha \cos(\sqrt{b}t_0), \quad \alpha_s = \alpha \sin(\sqrt{b}t_0), \quad (19)$$

account for the relative phase shift $\sqrt{b}t_0$ of each trajectory piece. One then estimates

$$\begin{aligned} \alpha &= \frac{\alpha_c}{\cos \arctan(\alpha_s/\alpha_c)}, \quad c = -\frac{4a}{\alpha^2}, \\ A &= \sqrt{\bar{a}b(2\langle x^2 \rangle - \alpha^2)}. \quad (20) \end{aligned}$$

The numerical error of fitting the approximate expression $\xi(t)$ to trajectory pieces $x_\pm(t)$ eventually exceeds the uncertainty of the driving noise $f(t)$ of a small amplitude $A \rightarrow 0$. One may even find a situation, in which the parameter A cannot be evaluated reliably through Eq. (20). For this reason we propose to use as a proxy the following formula

$$A = \max \left[\sqrt{\bar{a}b\epsilon}, \sqrt{\bar{a}b(2\langle x^2 \rangle - \alpha^2)} \right], \quad (21)$$

in which ϵ is the standard deviation of α over the sample of trajectories $x_\pm(t)$. This expression is motivated by the fact that, when the homogeneous term $\xi(t) \propto \alpha$ dominates the statistical variability of the data, the magnitude of $A \rightarrow 0$ cannot be inferred with a precision superior to $\sqrt{\bar{a}b\epsilon}$. We also adopt $\Delta A = \sqrt{\bar{a}b\epsilon}$ as the error estimate for A .

III. DIMENSIONAL ANALYSIS

In the system of units reduced by a time constant $b^{-1/2}$ and a length constant $\sqrt{-a/c}$, Eq. (1) takes a canonical form [3, Sec. 7.4 and 7.5]

$$\ddot{x} - \mu(1 - x^2)\dot{x} + x = \frac{A}{b\sqrt{-a/c}}\dot{w}, \quad (22)$$

in which the parameter $\mu = -a/\sqrt{b}$ controls the nonlinear character of the dynamics. The greater its value, the larger is the amplitude of the relaxation oscillations.

Two control parameters of Eq. (22) that are not fixed in the system of reduced units are μ and A . Without external driving the Van der Pol oscillator, which orbits around the origin of the phase space with the amplitude $\alpha = 2\sqrt{-a/c}$ in the harmonic potential $U(x) = bx^2/2$ [Eqs. (1) and (6)], has an energy scale

$$U(\alpha) = b\alpha^2/2 = 2\mu\sqrt{b^3/2}/c.$$

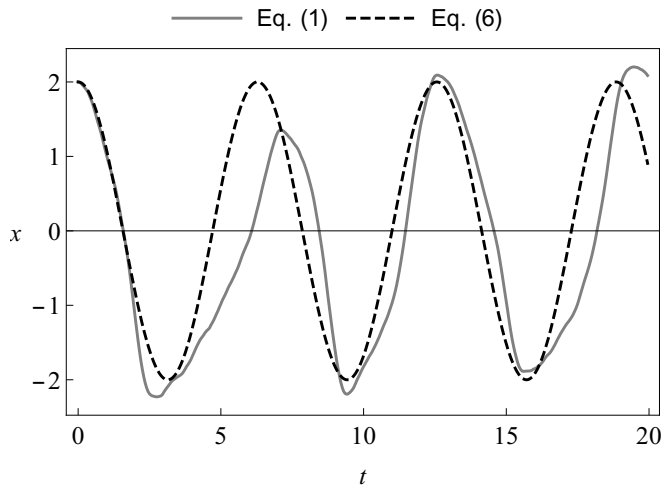


FIG. 1. Comparison of the theoretical Eq. (6) for the homogeneous term $\xi(t)$ with a simulation of Eq. (1): the system parameters are $\mu = 1$ and $A = 0.6$ in the reduced units (Sec. III); the initial conditions are $(x, \dot{x}) = (\alpha, 0)$. The analytical expression of $\xi(t)$ captures the overall trend of noisy oscillations of $x(t)$.

For increasingly large values of μ Eq. (6) becomes progressively less accurate. As a typical value we choose therefore $\mu = 1$. The techniques that we propose in the present paper should work also for $\mu > 1$, but their precision deteriorates for larger values of this parameter.

The energy scale of the external force $f(t) = A\dot{w}(t)$ is A^2/\sqrt{b} . One might therefore expect the small-force expansion Eq. (3) to hold for

$$A < \sqrt{\sqrt{b}U(\alpha)} = \alpha b^{3/4}/\sqrt{2} = b\sqrt{2\mu/c},$$

which relates the two control parameters of Eq. (22) A and μ .

IV. NUMERICAL RESULTS

To test the theoretical expressions of Sec. II A, we simulated Eq. (1) for selected values of the parameters μ and A (Sec. III). The computational details are summarized in Appendix B. Below we report the results of our simulations in the reduced units.

A comparison of the noisy oscillations of $x(t)$ with the theoretical expression for $\xi(t)$ is shown in Fig. 1. As a representative example we use the parameter values $\mu = 1$ and $A = 0.6$ and the initial conditions $(x, \dot{x}) = (\alpha, 0)$. The trajectory $\xi(t)$ approximates well the period of oscillations and the overall trend of $x(t)$.

For the same parameters as above, we compare the autocorrelation function $\chi(t)$ of the simulated time series $x(t)$ and the theoretical curve given by Eq. (16) in Fig. 2. The analytical expression of $\chi_\xi(t)$ predicts well the initial decay of the autocorrelation. However, a moderate

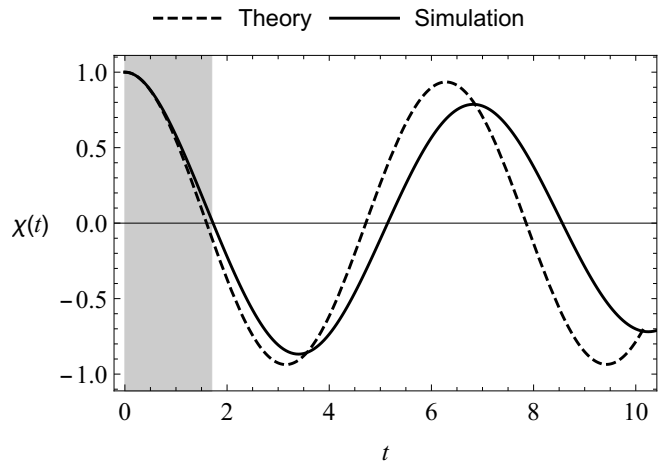


FIG. 2. Comparison of the theoretical Eq. (16) in which $\chi(t) \approx \chi_\xi(t)$ with the autocorrelation function of the simulated Eq. (1): the system parameters are $\mu = 1$ and $A = 0.6$ in the reduced units (Sec. III). The agreement is good in the shaded region selected by the criterion of Lagarkov and Sergeev (Sec. II B).

phase difference accumulates at longer times. Moreover, as explained in Sec. II B, $\chi(t)$ decays to zero with time to zero unlike the approximate Eq. (16). An amplitude difference between $\chi_\xi(t)$ and the actual autocorrelations therefore becomes evident in Fig. 2 at longer times.

The efficiency of the parametric-inference method we proposed in Sec. II B is demonstrated in Table I. The best results are obtained for a moderate level of noise $0.5 \lesssim A \lesssim 1.0$. The parameters a and b are inferred most reliably. Because relaxation oscillations have non-trivial statistics even in the absence of external forces, it is difficult to discriminate between the numerical errors of fitting approximate expressions and the uncertainty due to the driving noise. Our method estimates the ampli-

TABLE I. Inference of the Van der Pol oscillator's parameter values from time series of Eq. (1) that was simulated with $a = -1$, $b = 1$, $c = 1$ fixed and A varied in the range $[0, 1.2]$. The estimated parameter values are denoted by \hat{a} , \hat{b} , \hat{c} , and \hat{A} , respectively. The uncertainties are given by three standard errors of fitting for a and b , and by one standard deviation for c . The error ΔA is estimated as described in Sec II B.

\hat{A}	\hat{a}	\hat{b}	\hat{c}	\hat{A}
0.0	-1.1 ± 0.4	1.03 ± 0.02	1.0 ± 0.1	$(0.02)^*$
0.2	-1.1 ± 0.4	1.03 ± 0.01	1.0 ± 0.2	$(0.1)^*$
0.4	-1.1 ± 0.3	1.03 ± 0.01	1.0 ± 0.2	$(0.2)^*$
0.6	-1.1 ± 0.3	1.04 ± 0.01	1.1 ± 0.3	0.6 ± 0.4
0.8	-1.1 ± 0.2	1.04 ± 0.02	1.1 ± 0.5	1.0 ± 0.5
1.0	-1.1 ± 0.2	1.04 ± 0.02	1.2 ± 0.6	1.2 ± 0.6
1.2	-1.1 ± 0.2	1.04 ± 0.02	1.2 ± 0.8	1.5 ± 0.7

* Estimates evaluated by Eq. (21)

tude A of the stochastic force $f(t)$ only within its order of magnitude.

V. CONCLUSION

Using the Volterra series we have analyzed statistical features of a noisy Van der Pol equation. Perhaps surprisingly, its solution can be decomposed within the linear order of the driving force into two independent contributions: a deterministic part that describes relaxation oscillations, and a stochastic linear-response term. With the help of simple approximation schemes we showed that the deterministic contribution has a singular probability density, whereas the stochastic part can be described by a Gaussian process with a second-order autocorrelation function.

The inference method based on our analytical results allows us to estimate parameter values of the stochastic Van der Pol model from observed time series of oscillations for moderate levels of the driving noise. For small noise amplitudes only an order of magnitude can be determined due to insufficient accuracy of our simple approximations. More accurate approximation approaches exist, for example, the two-timing method [3, Sec. 7.6], and could be pursued to improve the precision of the analytical formulas.

APPENDICES

Appendix A: Statistical properties of noisy relaxation oscillations

Even in the absence of the external force $f(t)$ in Eq. (5), relaxation oscillations of the Van der Pol oscillator have nontrivial statistics. The steady-state probability distribution of the approximate homogeneous solution $x_0(t) \approx \xi(t)$ [Eq. (6)] obeys an arcsine law [20, Chapters 16 and 17]. Its probability density $p(\xi) \approx p(x_0)$ belongs to the family of beta distributions, with the support interval shifted by $-1/2$ and scaled by $4\sqrt{-a/c}$:

$$p(\xi) = \frac{d}{\pi d\xi} \left[\arcsin \left(\frac{\xi}{\alpha} \right) - \frac{\pi}{2} \right] = \frac{(\pi\alpha)^{-1}}{\sqrt{1 - \xi^2/\alpha}}. \quad (\text{A1})$$

The mean and the autocovariance function of $\xi(t)$ can be evaluated by time averaging

$$\langle \xi \rangle = \int_0^{2\pi/\sqrt{b}} \frac{\sqrt{b} ds}{2\pi} \xi(s) = 0, \quad (\text{A2})$$

$$\langle \xi(0)\xi(t) \rangle = \int_0^{2\pi/\sqrt{b}} \frac{\sqrt{b} ds}{2\pi} \xi(s)\xi(s+t) = \frac{\alpha^2}{2} \cos(\sqrt{b}t). \quad (\text{A3})$$

The probability density of ξ has two singularities at the ends of its support interval $\xi = \pm\alpha$. Histograms

of the time series $\xi(t)$ and $x(t)$ have two distribution modes near these points. In the companion paper [13] we have succeeded in fitting a bimodal probability density of the noisy Duffing oscillator to an approximate expression that was derived from a power series for the exponential family of random variables. This approach unfortunately fails however in the case of the noisy Van der Pol oscillator: such an expansion may not exist near the two singularities at which $p(x_0)$ tends to infinity.

For the probability density of $x_\xi(t)$ [Eq. (14)], regarded as the sum of two independent variables $\xi(t)$ and Gaussian variable $\gamma_\xi(t)$, there is no simple analytical expression. However the Fourier image $\eta(X_\xi)$ —the characteristic function of x_ξ for the reciprocal variable X_ξ —can be obtained in a closed form. Because $\gamma_\xi(t)$ is Gaussian, we have

$$\eta(X_\xi) = \langle e^{iX_\xi x_\xi} \rangle = J_0(\alpha X_\xi) \exp \left(\frac{A^2 X_\xi^2}{4ab} \right), \quad (\text{A4})$$

in which

$$J_0(\alpha X_\xi) = \int_0^{2\pi/\sqrt{b}} \frac{\sqrt{b} ds}{2\pi} e^{iX_\xi \xi(s)}$$

is the characteristic function of ξ and $J_0(\cdot)$ is the zeroth-order Bessel function of the first kind. The autocovariance of x_ξ is simply the sum of Eqs. (A3) and (16). In Fig. 3 we compare the empirical characteristic function of $x(t)$ (Appendix B) with Eq. (A4) for two representative examples. Our analytical expression for $\eta(X_\xi)$ is accurate at least for $X_\xi \lesssim \langle x \rangle^{-1/2}$ even for large noise amplitudes A . The theory is in excellent agreement with the simulations for $A \equiv 0$.

Appendix B: Simulation algorithm

In our computational experiments we use a companion system of Eq. (1) with $\mathbf{X} = (x, y) = (x, \dot{x})$:

$$\begin{cases} \dot{x} = y \\ \dot{y} = -(a + cx^2)y - bx + f(t) \end{cases}. \quad (\text{B1})$$

We adopt a second-order operator-splitting approach [21] for stochastic systems [13, 22, Appendix C], by decomposing the time-evolution operator \mathcal{T} as

$$\dot{\mathbf{X}} = \mathcal{T}\mathbf{X} = (\mathcal{T}_f + \mathcal{T}_y + \mathcal{T}_x)\mathbf{X}, \quad (\text{B2})$$

in which

$$\mathcal{T}_x = y\partial_x, \quad \mathcal{T}_y = -(a + cx^2)y\partial_y, \quad \mathcal{T}_f = (f - bx)\partial_y.$$

The formal solution of Eq. (B2) for a time step Δt

$$\mathbf{X}(t + \Delta t) = \exp(\mathcal{T}\Delta t)\mathbf{X}(t)$$

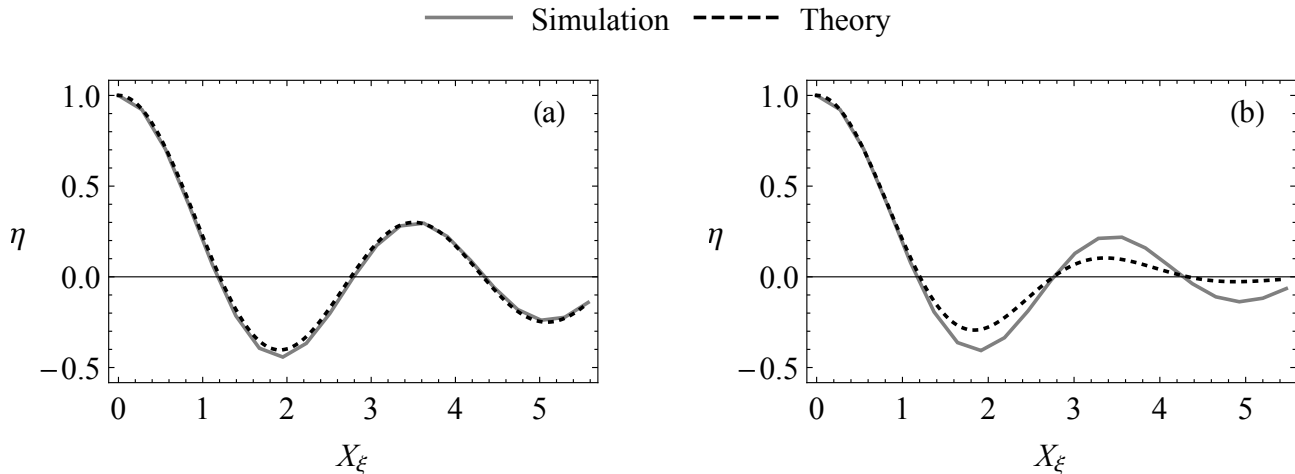


FIG. 3. Comparison of an empirical characteristic function for $x(t)$ from our simulations with the theoretical expression given by Eq. (A4); the system parameters are (a) $\mu = 1$, $A = 0.0$ and (b) $\mu = 1$, $A = 0.6$ in the reduced units (Sec. III). In these examples the theory is accurate at least for $X_\xi \lesssim \langle x^2 \rangle^{-1/2} \approx 0.7$.

can be approximated by

$$\begin{aligned} \exp[\mathcal{T}\Delta t + \mathcal{O}(\Delta t^2)] &= \exp\left(\frac{\mathcal{T}_x\Delta t}{2}\right) \exp\left(\frac{\mathcal{T}_y\Delta t}{2}\right) \\ &\times \exp(\mathcal{T}_f\Delta t) \exp\left(\frac{\mathcal{T}_y\Delta t}{2}\right) \exp\left(\frac{\mathcal{T}_x\Delta t}{2}\right). \end{aligned} \quad (\text{B3})$$

The action of individual operators of the form $\exp(\mathcal{L}\Delta t)$ is then determined by the differential equation

$$\dot{\mathbf{X}}(t) = \mathcal{L}\mathbf{X}(t) \Rightarrow \mathbf{X}(t + \Delta t) = \exp(\mathcal{L}\Delta t)\mathbf{X}(t). \quad (\text{B4})$$

The operators T_x , T_y , and T_f produce linear equations of the above type. The composite operator (B3) leads then to the following integration algorithm for Eq. (B2)

$$x(t + \Delta t/2) = x(t) + y(t)\Delta t/2, \quad (\text{B5})$$

$$\begin{aligned} y(t + \Delta t) &= y(t) \exp\{-[a + cx(t + \Delta t/2)^2]\Delta t\} \\ &- \exp\{-[a + cx(t + \Delta t/2)^2]\Delta t/2\} bx(t + \Delta t/2)\Delta t \\ &+ \exp\{-[a + cx(t + \Delta t/2)^2]\Delta t/2\} \int_t^{t+\Delta t} dt f(t), \end{aligned} \quad (\text{B6})$$

$$x(t + \Delta t) = x(t + \Delta t/2) + y(t + \Delta t)\Delta t/2. \quad (\text{B7})$$

For each value of the parameter A , the simulations reported in Sec. IV involved 5×10^5 time steps of a size $\Delta t = 0.01$ in the reduced units. Statistics were calculated from single trajectories sampled at time intervals of 0.05, which included 10^5 observations.

Appendix C: Correction of the linear-response formula

Equation (17) improves on Eq. (16) by replacing the effective friction parameter $\langle a_\xi \rangle = -a$ with \bar{a} [cf. Eqs. (7)–

(13)]. To obtain this correction, we first refine the approximation of the homogeneous term $x_0(t)$ by use of a variational Green-function approach.

The homogeneous Van der Pol Eq. (4) for $x_0(t)$ can be written as

$$\mathcal{L}_\omega x_0 = -a\dot{x}_0 - (b - \omega^2)x_0 - c\dot{x}_0x_0^2, \quad (\text{C1})$$

in which $\mathcal{L}_\omega = \partial_t^2 + \omega^2$ is a linear differential operator with a constant frequency parameter $\omega > 0$. As in the harmonic-balance method [16, Sec. 4.4] (Sec. II), we use the initial condition $(x, \dot{x}) = (\alpha, 0)$ with α left unspecified. The solution of Eq. (C1) must then satisfy

$$\begin{aligned} x_0(t) &= x_\omega(t) - \int_0^t g_\omega(t-s) \\ &\times [a\dot{x}_0(s) + (b - \omega^2)x_0(s) + c\dot{x}_0(s)x_0(s)^2] \\ &= \alpha \cos(\omega t) - \frac{\sin(\omega t)}{\omega} \int_0^t \cos(\omega s) \\ &\times [a\dot{x}_0(s) + (b - \omega^2)x_0(s) + c\dot{x}_0(s)x_0(s)^2] \\ &+ \frac{\cos(\omega t)}{\omega} \int_0^t \sin(\omega s) \\ &\times [a\dot{x}_0(s) + (b - \omega^2)x_0(s) + c\dot{x}_0(s)x_0(s)^2], \end{aligned} \quad (\text{C2})$$

in which $x_\omega(t) = \alpha \cos(\omega t)$ solves the equation $\mathcal{L}_\omega x_\omega = 0$, whereas $g_\omega(t) = \sin(\omega t)/\omega$ is the Green function associated with the operator \mathcal{L}_ω .

The values of $\alpha = 2\sqrt{-a/c}$ and $\omega = \sqrt{b}$ are inferred by requiring that $x_0(0) = x_0(2\pi/\omega)$ has a period $2\pi/\omega$ in Eq. (C2) with $x_0(t) \approx x_\omega(t)$. This result, which coincides with that of the harmonic-balance method [Eq. (6)], can be further improved by one Picard iteration: we insert $x_0(t) \rightarrow x_\omega(t)$ back into the right-hand side of Eq. (C2)

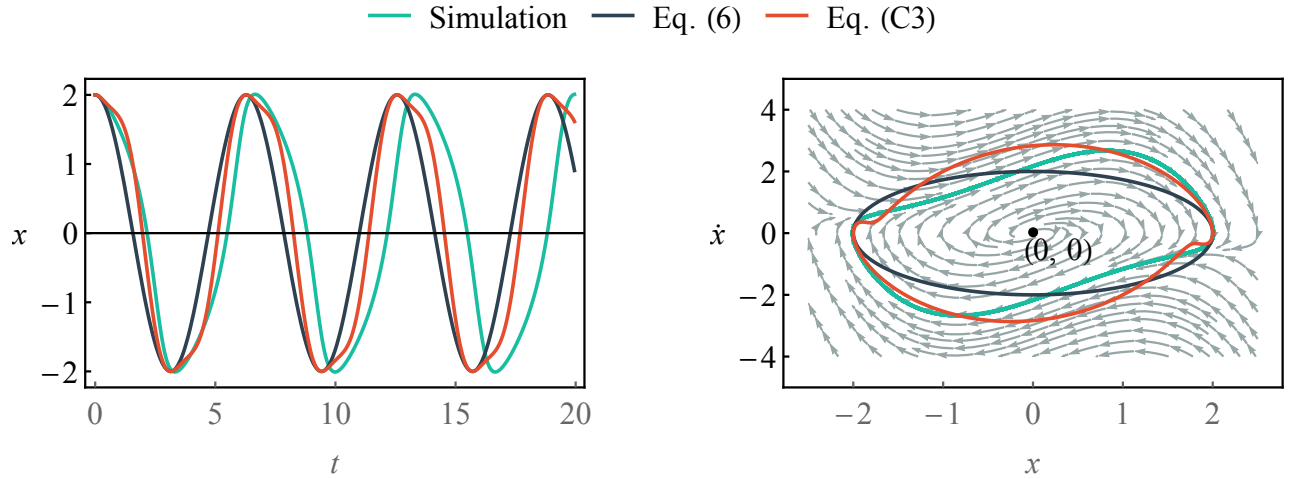


FIG. 4. Comparison of the approximate Eqs. (6) and (C3) with a simulation of the homogeneous Van der Pol oscillator Eq. (4) (Appendix B): (a) a limit-cycle trajectory with the initial conditions $(x_0, \dot{x}_0) = (2, 0)$; (b) the orbit of the oscillator's limit cycle in the phase space (x_0, \dot{x}_0) . The system parameters are $\mu = 1$ and $A = 0$. The two approximate expressions match well the simulated trajectory in panel (a) over a time interval of one period $t \lesssim 2\pi/\sqrt{b} \approx 6.28$. However, the asymmetric features of the oscillator's limit cycle are reproduced only by Eq. (C3). Equation (6) also underestimates the amplitude of the velocity oscillations $\dot{x}_0(t)$ in the phase space, see panel (b).

and complete the integration:

$$\begin{aligned} x_0(t) &\approx \bar{\xi}(t) \\ &= \alpha \left[\cos(\sqrt{b}t) + \frac{3\mu}{8} \sin(\sqrt{b}t) - \frac{\mu}{8} \sin(3\sqrt{b}t) \right]. \quad (\text{C3}) \end{aligned}$$

This iterative method resembles that of Refs. [23, 24], but is based on a different Piccard operator.

With $\bar{\xi}(t)$ substituted for $\xi(t)$, Eqs. (7)–(15) lead to

Eq. (17). In Fig 4 we compare the approximate Eqs. (6) and (C3) with a numerical solution of Eq. (4). Unlike $\xi(t)$, the curve $\bar{\xi}(t)$ reproduces asymmetric features of the trajectory $x_0(t)$. In phase space [Fig. (4)(b)] it is easy to see that Eq. (6) underestimates the amplitude of the velocity oscillations, whereas the orbit of Eq. (C3) is close to the numerical solution.

The sample variance $\langle x_0^2 \rangle \approx 2.1$ is slightly underestimated by $\langle \xi^2 \rangle = 2$ and overestimated by $\langle \bar{\xi}^2 \rangle \approx 2.3$. This difference leads to a larger value of the effective friction parameter \bar{a} in Eq. (17) than $-a$ in (16).

-
- [1] B. van der Pol, The London, Edinburgh, and Dublin Philosophical Magazine and Journal of Science **2**, 978 (1926).
- [2] J.-M. Ginoux and C. Letellier, Chaos: An Interdisciplinary Journal of Nonlinear Science **22**, 023120 (2012).
- [3] S. H. Strogatz, *Nonlinear Dynamics and Chaos: With Applications to Physics, Biology, Chemistry, and Engineering*, 2nd ed. (Avalon Publishing, 2014).
- [4] B. van der Pol, The London, Edinburgh, and Dublin Philosophical Magazine and Journal of Science **6**, 763 (1928).
- [5] B. van der Pol, Acta Medica Scandinavica **103**, 76 (1940).
- [6] R. FitzHugh, Biophysical Journal **1**, 445 (1961).
- [7] J. Nagumo, S. Arimoto, and S. Yoshizawa, Proceedings of the IRE **50**, 2061 (1962).
- [8] E. Izhikevich and R. FitzHugh, Scholarpedia **1**, 1349 (2006).
- [9] R. Alonso, F. Goller, and G. B. Mindlin, Physical Review E **89** (2014), 10.1103/PhysRevE.89.032706.
- [10] G. B. Mindlin, Chaos: An Interdisciplinary Journal of Nonlinear Science **27**, 092101 (2017).
- [11] A. A. Cherevko, A. V. Mikhaylova, A. P. Chupakhin, I. V. Ufimtseva, A. L. Krivoshapkin, and K. Y. Orlov, Journal of Physics: Conference Series **722**, 012045 (2016).
- [12] A. A. Cherevko, E. E. Bord, A. K. Khe, V. A. Panarin, and K. J. Orlov, Journal of Physics: Conference Series **894**, 012012 (2017).
- [13] R. Belousov, F. Berger, and A. J. Hudspeth, Physical Review E **99** (2019), 10.1103/physreve.99.042204.
- [14] M. Schetzen, *The Volterra and Wiener Theories of Nonlinear Systems* (Krieger Pub., 2006).
- [15] W. J. Rugh, *Nonlinear System Theory: The Volterra/Wiener Approach* (Johns Hopkins University Press, 1981).
- [16] D. Jordan and P. Smith, *Nonlinear Ordinary Differential Equations: An Introduction for Scientists and Engineers: An Introduction for Scientists and Engineers* (OUP Ox-

- ford, 2007).
- [17] R. Belousov and E. G. D. Cohen, *Physical Review E* **94** (2016), 10.1103/PhysRevE.94.062124.
- [18] S. Chandrasekhar, *Rev. Mod. Phys.* **15**, 1 (1943).
- [19] A. N. Lagar'kov and V. M. Sergeev, *Soviet Physics Uspekhi* **21**, 566 (1978).
- [20] N. Balakrishnan and V. B. Nevzorov, *A Primer on Statistical Distributions* (John Wiley & Sons, 2004).
- [21] M. Tuckerman, B. J. Berne, and G. J. Martyna, *The Journal of Chemical Physics* **97**, 1990 (1992).
- [22] R. Belousov, E. G. D. Cohen, and L. Rondoni, *Physical Review E* **96** (2017), 10.1103/PhysRevE.96.022125.
- [23] S. A. Khuri and A. Sayfy, , 9 (2017).
- [24] M. Abukhaled, *Journal of Computational and Nonlinear Dynamics* **12**, 051021 (2017).